Finite-Element Analysis and Design of Binder Wraps for Automobile Sheet Metal Parts Using Surface Boundary Condition

I.S. Song, D.J. Yoo, J.W. Yoon, D.Y. Yang, H. Huh, and J.H. Lee

The forming of automobile sheet metal parts in a draw die consists of clamping a blank by binders to form a binder wrap and drawing the blank into the final part. This paper proposes a numerical method to calculate the binder wrap. A blank is composed of two regions: the contact region with the die face and the noncontact region of the die cavity. In this study, surface boundary condition is suggested for calculating the configuration of the binder wrap. Surface boundary condition means that the three-dimensional geometric data of the die face are used as the base for the displacement boundary condition of the finite-element analysis. To verify the validity of the proposed method, the binder wraps of complicated automobile parts, including a front fender and a trunk lid, are analyzed.

Keywords

automobile sheet metal parts, binder wrap, finite-element analysis, sheet metal working, surface boundary condition

1. Introduction

SHEET METAL forming using deep drawing dies consists of two stages. First, the initial sheet blank is held by the blank holder or the binder surfaces, and then it is further formed into the final shape of the part. In the present work, a numerical method to compute a binder wrap as an initial sheet blank for further forming is presented and applied to several practical examples in automobile manufacture.

The prediction of initial sheet blank deformation in binder holding is an indispensable step of sheet metal forming analysis, providing such basic data as prediction of initial punch contact, computation of draw depth and die face design, and so on. Obtaining an exact solution for a binder wrap involves various factors, including contact and friction between the sheet material and the binder or, more specifically, between the sheet material and the beads. However, solution convergency, computational time, and other practical matters demand a more approximate and simplified approach.

Thus far, two types of approaches have been reported for binder wrap analysis: the surface interpolation method and the finite-element method (FEM) based on elastic deformation. In surface interpolation, binder wraps are generated purely in the manner of computer-aided design (CAD) surface generation by utilizing the punch opening line and binder surfaces as basic data (Ref 1-3). The method has the advantage of fast computation time and considerably exact solution, provided that the binder surfaces are relatively simple. When the binder surfaces are complicated with compound curvatures, solution becomes less accurate, and the sheet thickness and material properties are not considered at all.

I.S. Song, D.J. Yoo, J.W. Yoon, D.Y. Yang, and **H. Huh,** Department of Mechanical Engineering, KAIST, Taejon, Korea; **J.H. Lee,** Stamping Tool Manufacturing Department, Hyundai Motors Company, Ulsan, Korea

The finite-element method has been applied in order to overcome these drawbacks. Tang (Ref 4, 5) developed an analysis model by successively increasing the curvature of a flat plate. A proprietary code (Ref 6) was used in the numerical calculations. The model developed by Mital (Ref 7) allowed the blank to flow into the die cavity while the bottom edge of the blank was pivoted using the commercial code NASTRAN. Chen (Ref 8) proposed an iterative method to solve the binder wrap by using noncompatible eight-node quadrilateral elements and applied it to a practical problem. He confirmed the solution accuracy by computing for a known problem with an exact solution (Ref 9).

In reality, some part of a binder wrap may undergo plastic deformation, and the entire region should be computed by elastic-plastic FEM. This method requires a lengthy computation that is impractical for large automobile parts and does not render any difference in the shape of binder wraps. Therefore, elastic FEM is more effective in such applications. The gravity effect can be safely ignored, because the weight of the sheet has little influence on blank deformation.

In the present work, an FEM to compute general binder wraps is proposed using surface boundary conditions and is applied to actual automobile sheet metal parts.

2. Definition of Binder Surface

As Fig. 1 illustrates, the sheet metal part surface on the corresponding die surface is complicated and cannot be described in terms of simple analytic surfaces (circle, plane, etc.). In computing a binder wrap for an automobile sheet panel, the die face should be defined in terms of basic patch representation (Ref 10):

$$\mathbf{r}(u,v) = x(u,v)\mathbf{i} + y(u,v)\,\mathbf{j} + z(u,v)\,\mathbf{k} \quad (0 \le u, v \le 1) \quad \text{(Eq 1)}$$

The present analysis uses a third-order Ferguson surface patch that is widely employed in industrial practice. A general third-order Ferguson curved surface patch is expressed as:

$$\mathbf{r}(u,v) = [\alpha_0(u)\,\mathbf{r}(0,0) + \alpha_1(u)\,\mathbf{r}(1,0) + \beta_0(u)\,\mathbf{r}_u(0,0) + \beta_1(u)\,\mathbf{r}_u(1,0)]\,\alpha_0(v) + [\alpha_0(u)\,\mathbf{r}(0,1) + \alpha_1(u)\,\mathbf{r}(1,1) + \beta_0(u)\,\mathbf{r}_u(0,1) + \beta_1(u)\,\mathbf{r}_u(1,1)]\,\alpha_1(v) + [\alpha_0(u)\,\mathbf{r}_v(0,0) + \alpha_1(u)\,\mathbf{r}_v(1,0)]\beta_0(v) + [\alpha_0(u)\,\mathbf{r}_v(0,1) + \alpha_1(u)\,\mathbf{r}_v(1,1)]\beta_1(v) \quad \text{(Eq 2)}$$

where u and v are variables ($0 \le u, v \le 1$), $\mathbf{r}$ is the position vector at four corner points of a patch, $\mathbf{r}_u$ is the tangential vector in the u-direction at four corner points of a patch, and $\mathbf{r}_v$ is the tangential vector in the v-direction at four corner points of a patch. In addition,

$$\alpha_0(u) = 1 - 3u^2 + 2u^3 \qquad \alpha_0(v) = 1 - 3v^2 + 2v^3$$
$$\alpha_1(u) = 3u^2 - 2u^3 \qquad \alpha_1(v) = 3v^2 - 2v^3$$
$$\beta_0(u) = u - 2u^2 + u^3 \qquad \beta_0(v) = v - 2v^2 + v^3$$
$$\beta_1(u) = -u^2 + u^3 \qquad \beta_1(v) = -v^2 + v^3$$

The foregoing Ferguson patches form a curved surface, and the entire binder face is made up of a combination of such surfaces. In commercial CAD systems (e.g., CATIA), higher-order patches (fifth order, seventh order, etc.) are often used to describe highly curved surfaces. In the present work, however, to simplify matters somewhat, the data from the CATIA system are converted to third-order Ferguson patches for binder wrap analysis.

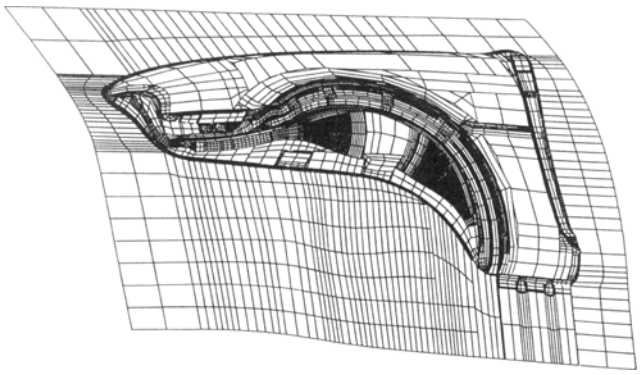

Fig. 1 Arbitrarily shaped tool surface

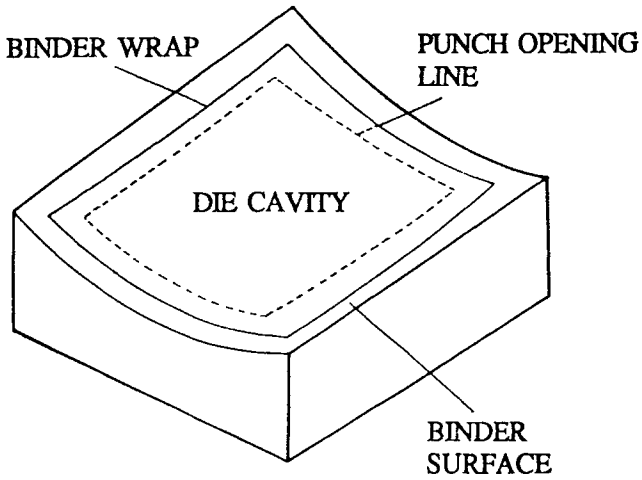

Fig. 2 Binder wrap and draw die

3. Surface Boundary Condition

In the forming of panel-like sheet metal (Fig. 2), the peripheral region of the sheet blank is held by the binder face. The binder wrap can be divided into two regions: a contact region held between the binder faces outside the punch opening line and a free surface region inside the punch opening line. In solving a binder wrap, the deformed shapes of the contact region and the free surface region are computed from the given boundary condition. In the present work, the binder wraps corresponding to general binder surfaces are computed using the surface boundary condition.

In applying the surface boundary condition, nodal points are generated for all the surface elements of the initial sheet blank. Vertical lines are drawn from these nodal points along the pressing direction (Fig. 3). The corresponding displacements at all intersecting points between the vertical lines and the binder surface are determined and are used for the displacement boundary condition in the finite-element analysis of initial sheet deformation during the binding-holding stage. The surface boundary condition determined in this way is a basic boundary condition for computation of a binder wrap and plays an important role in exact estimation.

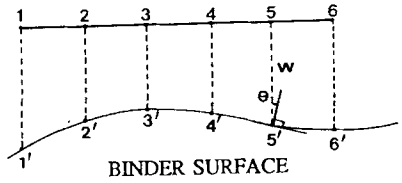

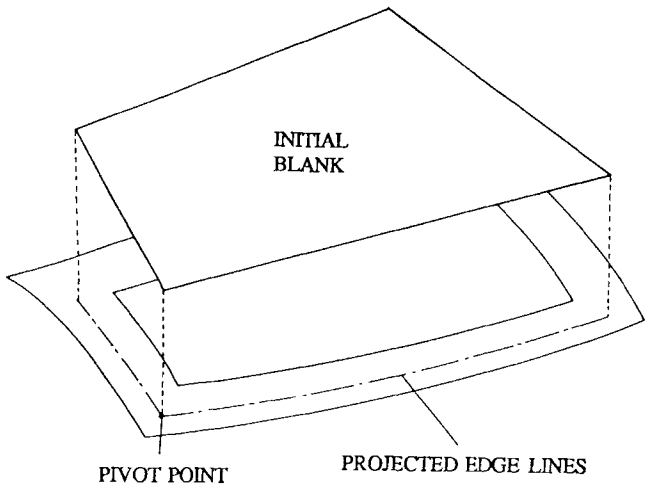

Fig. 3 Basic concept of surface boundary condition

4. Intersection between Line Vectors and the Binder Surface

The binder surface is a compound surface composed of a number of surfaces that are again made up of multiple patches. In order to project all the surface nodal points of the initial sheet blank into the binder surface, two basic steps are required for treatment of surface boundary condition before computing the binder wrap. First, a specific patch is selected that intersects with a line vector directing in the pressing direction from an arbitrary nodal point. Then an intersecting point is found between the line vector and the selected patch.

4.1 *Determination of a Patch Intersected by the Line Vector*

Either of two methods generally is used to select a patch intersected by the line vector. One method is to generate a polyhedron for each patch of a curved surface and to check whether the line vector intersects with the polyhedron. In the other method (Ref 11), a vector criterion using the line vector and the boundary curves of a patch is employed. In the present work, an improved technique that reflects all the advantages of the foregoing method is proposed for the sake of computational efficiency and reliability. Point O is on the sheet material, and point C is located at some distance toward the pressing direction. The boundary curves of a patch of the binder face are simply expressed by straight lines. Then the searching problem of a patch is solved by the intersection of a boundary line with a plane that includes the vector **OC**, a simplified approach that greatly reduces computation time. After the search for an intersecting patch, an intersecting point between a boundary curve and the intersecting plane is found by the Newton-Raphson method by introducing an initial guess as an intersection between a line and the plane corresponding to the curved boundary of an intersecting patch, which improves the convergency. After determining the intersecting points A and B (Fig. 4), the possibility of intersection between a line and a specific patch is checked by the following vector criterion:

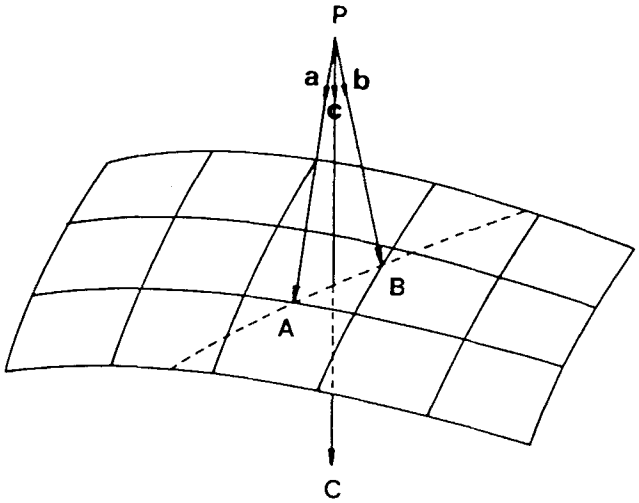

Fig. 4 Search to determine the patch intersected by vector **OC**

$$(\mathbf{OA} \times \mathbf{OC}) \cdot (\mathbf{OB} \times \mathbf{OC}) < 0 \qquad \text{(Eq 3)}$$

4.2 *Determination of an Intersection Point between a Line Vector and a Patch*

An intersection point between a line vector and a patch can be determined by the following nonlinear equation, which includes three variables from the general expressions of a line vector and a general patch:

$$\mathbf{F}(u,v,\lambda) = \mathbf{r}_0 + \lambda\mathbf{n} - \mathbf{r}(u,v) = 0 \qquad \text{(Eq 4)}$$

where $\mathbf{r}_0$ is the starting point of a line vector, $\mathbf{n}$ is a unit vector in the line direction, and $\mathbf{r}(u,v)$ is a polynomial function of a patch. In order to determine u, v, and λ, the following iterative equation is obtained from Eq 4:

$$\begin{bmatrix} u_{i+1} \\ v_{i+1} \\ \lambda_{i+1} \end{bmatrix} = \begin{bmatrix} u_i \\ v_i \\ \lambda_i \end{bmatrix} - J^{-1} \begin{bmatrix} F_1(u_i,v_i,\lambda_i) \\ F_2(u_i,v_i,\lambda_i) \\ F_3(u_i,v_i,\lambda_i) \end{bmatrix} \qquad \text{(Eq 5)}$$

where **J** is a Jacobian matrix defined as:

$$J = \begin{bmatrix} \frac{\partial F_1}{\partial u} & \frac{\partial F_1}{\partial v} & \frac{\partial F_1}{\partial \lambda} \\ \frac{\partial F_2}{\partial u} & \frac{\partial F_2}{\partial v} & \frac{\partial F_2}{\partial \lambda} \\ \frac{\partial F_3}{\partial u} & \frac{\partial F_3}{\partial v} & \frac{\partial F_3}{\partial \lambda} \end{bmatrix}$$

and F_1, F_2, and F_3 are components of $\mathbf{F}(u,v,\lambda)$ in the x, y, and z directions, respectively, of Eq 4. A solution satisfying Eq 5 can be obtained through iterative computation with an appropriate initial guess. If the initial guess is inappropriate, either no converged solution is obtained or the computed values of parameters u and/or v will be out of the range between 0 and 1, leading to a meaningless solution.

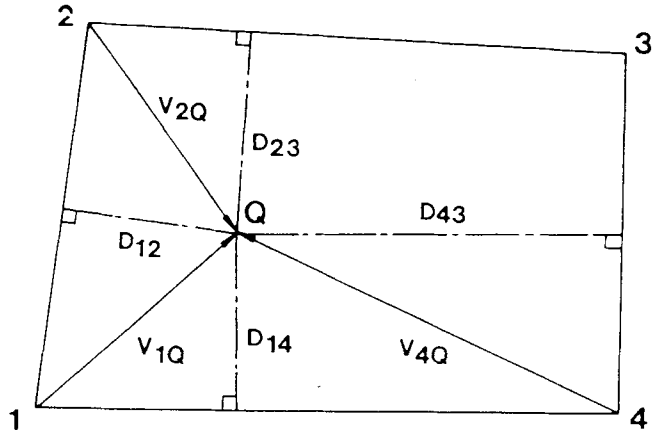

Fig. 5 Method used to obtain an initial guess for parameters u and v

The initial guess is obtained from the geometrical relation between four corner points and the point Q (Fig. 5) projected perpendicularly from the plane containing three corner points (e.g., points 1, 2, and 4) (Ref 11):

$$u = \frac{V_{2Q} \cdot V_{23}}{|V_{23}|^2} \quad \text{if } \mathbf{D}_{23} < \mathbf{D}_{14}$$

$$v = \frac{V_{1Q} \cdot V_{12}}{|V_{12}|^2} \quad \text{if } \mathbf{D}_{12} < \mathbf{D}_{43}$$

$$u = \frac{V_{1Q} \cdot V_{14}}{|V_{14}|^2} \quad \text{if } \mathbf{D}_{14} < \mathbf{D}_{23}$$

$$v = \frac{V_{4Q} \cdot V_{43}}{|V_{43}|^2} \quad \text{if } \mathbf{D}_{43} < \mathbf{D}_{12} \qquad \text{(Eq 6)}$$

5. Calculation of the Binder Wrap

The present FEM analysis employs four-noded plate elements (Fig. 6). The plate element has three translational degrees of freedom as well as three rotational degrees of freedom for each nodal point. The initial blank shape can be formed by a single patch, but in general it may consist of multiple patches. In this study, the mesh is generated automatically for a general polygonal shape of the initial blank.

All the nodal points of the finite element are projected onto the binder surface for treatment of surface boundary condition, and then the displacements (u, v, w, θ_x, θ_y, θ_z) for each intersection point are found in order to apply them as boundary conditions for FEM analysis. The computational procedure is illustrated schematically in Fig. 7.

6. Computational Examples

6.1 *Comparison of FEM and Surface Interpolation*

To check its validity and practical applicability, the present method of binder wrap analysis was compared with the surface interpolation method. Binder wrap analyses were carried out by both methods for a test example as shown in Fig. 8. From the computational results of Fig. 8(b) and (c) both methods render similar deformation patterns. However, in the surface interpolation method the sheet material thickness and mechanical properties such as Young's modulus and Poisson's ratio are not taken into account, and the computed configuration is rather different from the actual deformed configuration. The FEM analysis gives more relevant results that approximate the real phenomenon.

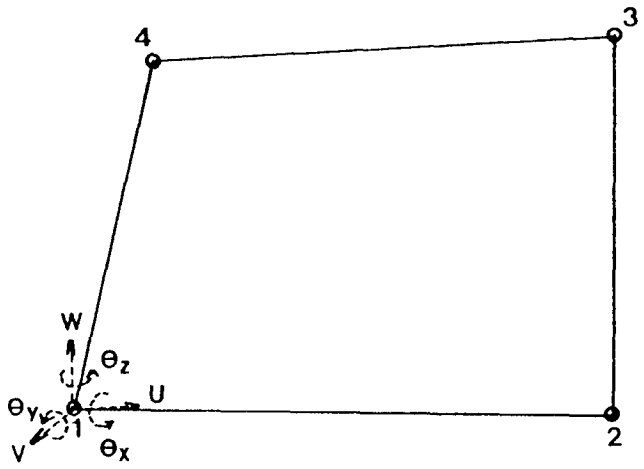

Fig. 6 Finite-element model (four-node plate element)

6.2 *Binder Wrap Analysis of a Trunk Lid*

A binder wrap analysis was carried out for a trunk lid of an automobile by elastic FEM using four-node plate elements. Sheet thickness was 1 mm, Young' modulus was 200 GPa, and Poisson's ratio was 0.3.

Figure 9(a) shows the binder surface for a trunk lid and the initial sheet blank. Because the trunk lid is symmetrical, only the right half was subjected to the analysis. Figure 9(b) shows the computed binder wrap together with the binder surface. In Fig. 9(c), only the computed binder wrap is presented. The binder surface used for computation consisted of 19 curved surfaces. For the finite-element mesh, 420 four-node plate elements were used.

6.3 *Binder Wrap Analysis of a Front Fender*

Another complicated example of an automobile sheet metal part was subjected to binder wrap analysis. Figure 10(a) shows the binder surface of an automobile front fender and the initial

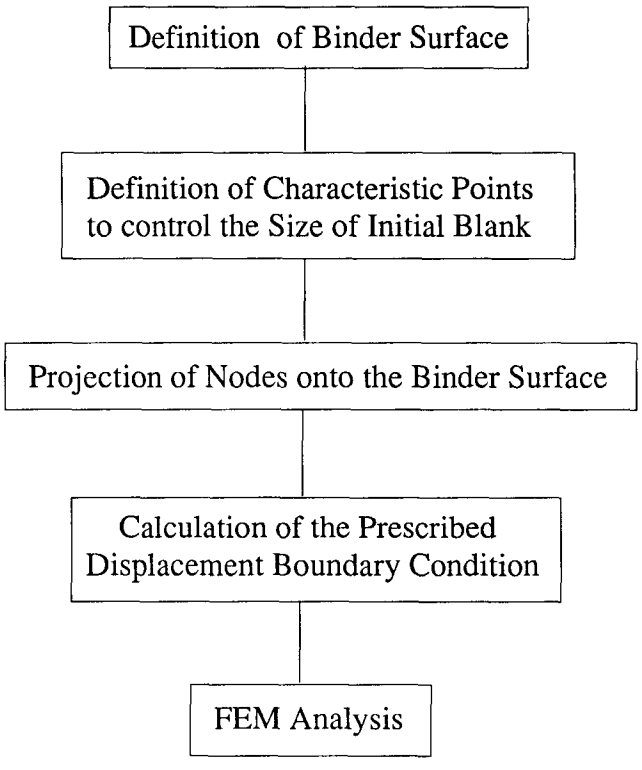

Fig. 7 Flow chart of computational procedure

sheet blank. The binder surface was a composite surface consisting of 38 curved surfaces and was constructed from CAD data given in CATIA format. The initial sheet blank was designed so that its boundary conformed to the boundary of the binder surface with sufficient holding of the surface. The finite-element mesh consisted of 768 elements. Figures 10(b) and (c) show the binder wrap surface and the computed binder wrap. The computed binder wrap gives a very smooth curved surface construction from the given surface boundary condition suggested in the present work.

7. Conclusions

A method of binder wrap analysis by elastic FEM has been proposed using the surface boundary condition for analysis of a general binder wrap. The curved surface boundary condition is used as a displacement boundary condition for elastic FEM analysis. Binder wrap analyses have been carried out for actual automobile panels, and the effectiveness of the present method of analysis has been confirmed from the computation results. The method enables the computation of initial contact position,

Nomenclature

$\mathbf{J}$	Jacobian matrix for the iterative procedure of Newton's method
$\mathbf{n}_{ij}$	normal vector at each node
$\mathbf{r}$	position vector at four corner points of a patch
$\mathbf{r}_u$	tangential vector in the u-direction at four corner points of a patch
$\mathbf{r}_v$	tangential vector in the v-direction at four corner points of a patch
u, v	two parameters of a parametric patch ($0 \le u \le 1, 0 \le v \le 1$)
$\mathbf{U}_{ij}, \mathbf{V}_{ij}$	tangent vectors in u- and v-directions, respectively, at each node
α_i, β_i	cubic blending functions used in describing a patch
λ	length of a line vector

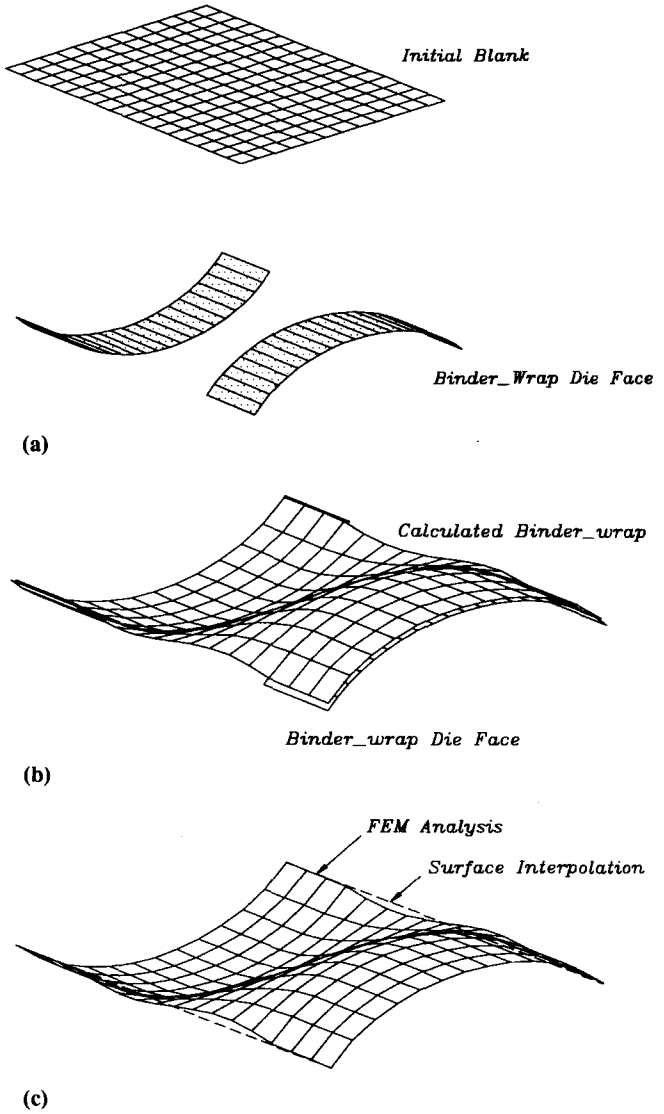

Fig. 8 Binder wrap analysis of test example to show the difference between FEM and surface interpolation. (a) Initial state. (b) Final state. (c) Calculated binder wrap

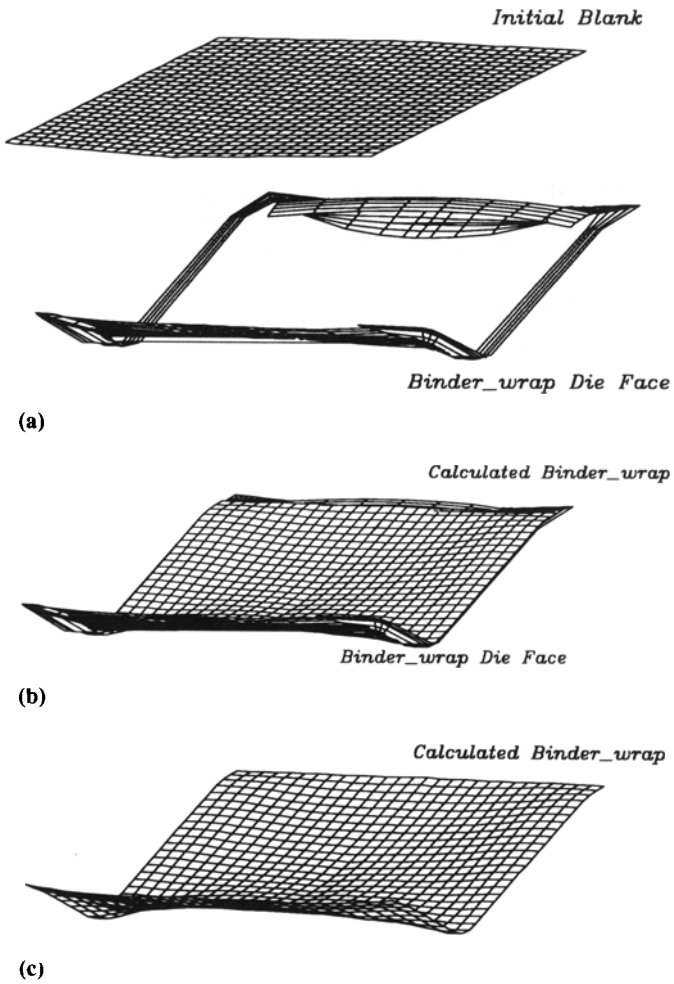

Fig. 9 Binder wrap analysis of trunk lid. (a) Initial state. (b) Final state. (c) Calculated binder wrap

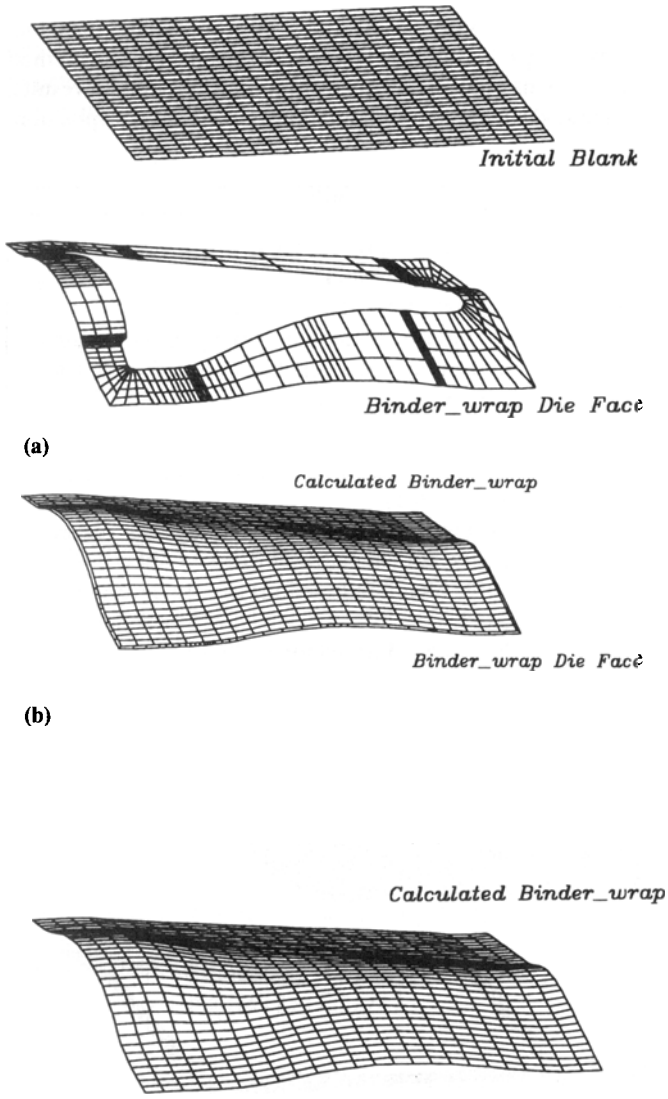

Fig. 10 Binder wrap analysis of front fender. (a) Initial state. (b) Final state. (c) Calculated binder wrap

approximate prediction of buckling and wrinkle formation during binder clamping, and material savings through minimization of drawing depth. Thus, the binder wrap analysis can be effectively used for construction of basic data for further forming analysis.

In future work, however, the present analysis should be verified through comparison with the experiment. An advanced binder wrap analysis is still required in which the gravity effect of the blank material at the initial state is included, with proper consideration of friction and contact treatment.

References

1. I. Okamoto, A. Takahashi, H. Sugiura, T. Hiramatsu, N. Yamada, and T. Mori, Computer Aided Design and Evaluation System for Stamping Dies in Toyota, Proc. SAE Conference, SAE, Feb 29-Mar 4, 1989, p 579-589
2. I.D. Faux and M.J. Pratt, *Computational Geometry for Design and Manufacturing*, E. Harwood, Ltd., England, 1979
3. G. Jun, Y.J. Yoo, and J.W. Lee, Development of KIA Die Face CAD/CAE System, *Trans. KSAE,* Vol 12 (No. 5), 1990, p 14-18
4. S.C. Tang, Computational Prediction of the Deformed Shape of a Draw Blank during the Binder-Wrap Stage, *J. Appl. Met. Work.,* Vol 1 (No. 3), 1980, p 22-29
5. S.C. Tang, Verification and Applications of a Binder Wrap Analysis, *Computer Modeling of Sheet Metal Forming Process,* N.M. Wang and S.C. Tang, Ed., TMS, 1986, p 193-203
6. S.C. Tang, "Elasto-Plastic and Large Deflection Analysis of Thin Shell by the Flow Theory of Plasticity," Paper No. 770590, SAE Publication P-71, Society of Automotive Engineers, 1977
7. N.K. Mital, Prediction of Binder Wrap in Sheet Metal Stamping Using Finite Element Method, *Proc. Int. Conf. Computer in Engineering,* American Society of Mechanical Engineers, 1983, p 71-77
8. K.K. Chen, A New Finite Element Method for Binder Wrap Calculation, *J. Mater. Shaping Technol.,* Vol 5, 1987, p 107-116
9. K.K. Chen, Evaluation of a Finite Element for Calculation Binder Wrap Surfaces in Sheet Metal Forming Analysis, *Finite Elem. Anal. Des.,* Vol 5, 1989, p 57-71
10. I.D. Faux, *Computational Geometry for Design and Manufacture,* M.J. Pratt, 1979
11. P.K. Scherrer and B.M. Hillberry, Determining Distance to a Surface Represented in Piecewise Fashion with Surface Patches, *Comput.-Aided Des.,* Vol 10 (No. 5), 1978, p 320-324